

Draft & Verify: Lossless Large Language Model Acceleration via Self-Speculative Decoding

Anonymous ACL submission

Abstract

We present a novel inference scheme, self-speculative decoding, for accelerating Large Language Models (LLMs) without the need for an auxiliary model. This approach is characterized by a two-stage process: drafting and verification. The drafting stage generates draft tokens at a slightly lower quality but more quickly, which is achieved by selectively skipping certain intermediate layers during drafting. Subsequently, the verification stage employs the original LLM to validate those draft output tokens in one forward pass. This process ensures the final output remains *identical* to that produced by the unaltered LLM. Moreover, the proposed method requires no additional neural network training and no extra memory footprint, making it a plug-and-play and cost-effective solution for inference acceleration. Benchmarks with LLaMA-2 and its variants demonstrated a speedup up to $1.99\times$.¹

1 Introduction

Transformer-based Large Language Models (LLMs), such as GPT-3/4, PaLM, and LLaMA, have been widely adopted in various real-world applications (Bommasani et al., 2021; Liang et al., 2022; Brown et al., 2020; Min et al., 2022; Chan et al., 2022; Touvron et al., 2023). However, their inference costs have raised significant concerns, especially for latency-sensitive scenarios (Pope et al., 2022). The main efficiency bottleneck is the *autoregressive decoding* process. This process decodes each output token sequentially, leading to a high number of Transformer calls; furthermore, each Transformer call is typically memory bandwidth-bound, resulting in low computation utility and thus longer wall-clock time (Shazeer, 2019). For instance, decoding 128 tokens autoregressively using LLaMA-2-13B on

¹Code is available at <https://openreview.net/attachment?id=ACC2nQYzPYS&name=software>, and will be released with the Apache-2.0 License.

an A100 GPU can take up to $100\times$ longer than a sequence-level forward pass on the same number of tokens, highlighting the substantial inefficiency inherent in the current decoding process.

Established model compression techniques such as quantization (Han et al., 2015), pruning (Molchanov et al., 2016), and distillation (Hinton et al., 2015) have been employed to alleviate these costs. While these solutions have proven extremely effective, they usually require changing the model architecture, changing the training procedure, re-training or fine-tuning the models, and do not maintain identical outputs.

In parallel to model compression, *speculative execution* is being explored to accelerate the autoregressive decoding process (Leviathan et al., 2023; Chen et al., 2023). These methods train an auxiliary **draft model** that can quickly generate some draft output tokens. Subsequently, the original LLM, referred to as the **verify model**, then checks the acceptability of these draft tokens with one single forward pass. This verification step ensures that the outputs are derived from the original LLM’s probability distribution.

However, an essential issue of existing speculative execution methods is the need to identify or train a suitable draft model that can generate outputs consistent with the verify model. It becomes more tricky when the LLM is already a fine-tuned model, e.g. LLaMA-2-Chat (Touvron et al., 2023), CodeLLaMA (Rozière et al., 2023). How to find or train a draft model that can effectively mimic the outputs of such a tailored model is a formidable task, with no straightforward or guaranteed solutions. Furthermore, the introduction of an additional draft model escalates the GPU memory overhead, increasing deployment challenges particularly on devices with restricted memory capacity.

In this paper, we present *self-speculative decoding*, a novel approach to accelerate the inference of LLMs. This method builds on the principles of

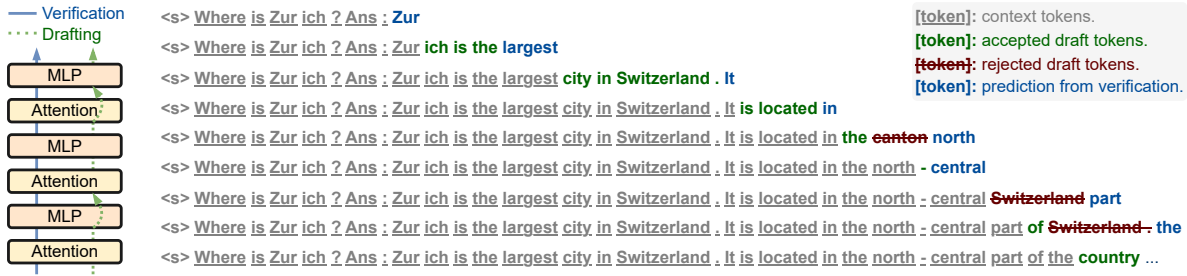


Figure 1: Visualization of the self-speculative decoding process. The verification stage evaluates all drafted tokens in a single forward pass, with accepted tokens marked in green and rejected tokens highlighted in red. Each verification step also predicts one more token, which is denoted in blue.

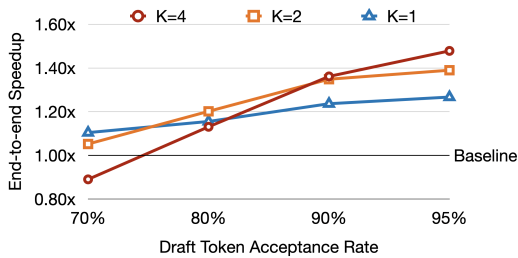


Figure 2: Impact of the number of draft tokens (K) and acceptance rate on end-to-end speedup. The draft model is assumed to be $2\times$ faster than the verify model.

speculative execution, but with a unique twist: it utilizes one LLM for both drafting and verification stages. The key insight driving our approach is the observation that skipping certain layers in LLMs does not significantly compromise the generation quality (Liu et al., 2023). As such, by selectively bypassing some intermediate layers, we can use the LLM itself to generate draft tokens. These tokens are then verified by the original LLM in a single forward pass. Figure 1 illustrates this two-stage decoding process. The blue arrow indicates the inference path of the original model, while the green arrow depicts the inference path during the drafting stage. Notably, both inference paths share the same model so we do not need a standalone draft model with extra memory overhead.

Implementing self-speculative decoding poses two main challenges: (a) determining which layers and the number of layers to skip during drafting, and (b) deciding the timing to stop generating draft tokens. To tackle the first challenge, we formulate it as an optimization problem, which accepts the combinations of layers to bypass as input and aims to minimize the average inference time per token. We employ Bayesian optimization (Jones et al., 1998) to solve this problem. The optimization is performed offline at the model level, and the searched

layer combinations are fixed. The second challenge pertains to determining the optimal number of draft tokens (K) to generate. As shown in Figure 2, the choice of K significantly influences the end-to-end speedup: for an acceptance rate below 80%, $K = 1$ is optimal, and for rates above 80%, a larger K is necessary. This observation underscores that a static K is not universally applicable. To tackle this variability, we introduce an adaptive draft-exiting mechanism, which stops generating draft tokens once its confidence level drops below a threshold. This intervention prevents unnecessary computation and potential discard of additional draft tokens, thereby enhancing efficiency.

To summarize, our main contributions are: (1) *Inference scheme*: we propose self-speculative decoding, a practical, plug-and-play solution for inference acceleration that does not require further neural network training and avoids additional memory overhead; (2) *Optimization strategies*: we adopt Bayesian optimization to select which layers to skip during drafting and propose a simple yet effective method to adaptively determine the number of draft tokens; (3) *Evaluation*: we evaluate our method on text summarization and code generation tasks, and the experimental results indicate that our method can achieve up to $1.99\times$ in end-to-end speedup.

2 Related Work

Transformer-based LLM inference. As LLMs continue to evolve rapidly, we are seeing a surge of systems specifically engineered for LLM inference, including Faster Transformer (NVIDIA), Orca (Yu et al., 2022), LightSeq (Wang et al., 2021), PaLM inference (Pope et al., 2022), TurboTransformers (Fang et al., 2021), Deepspeed Inference (Am-inabadi et al., 2022), FlexGen (Sheng et al., 2023), Text Generation Inference (HuggingFace, 2023), etc. The token generation phase typically takes up

the majority of the end-to-end inference time compared to the prompting encoding phase. Despite the introduction of system optimizations by those state-of-the-art systems to improve the inference speed, there is still a gap in the careful co-design of algorithms and systems. This is necessary to fully harness the potential of hardware efficiency during LLM inference computation.

Model Compression. Various model compression methods have been studied for model inference. For example, quantization (Han et al., 2015; Jacob et al., 2018; Nagel et al., 2019; Zhao et al., 2019; Yao et al., 2022; Park et al., 2022; Dettmers et al., 2022; Xiao et al., 2022; Frantar et al., 2022), pruning or sparsification (Molchanov et al., 2016; Liu et al., 2018; He et al., 2019; Hoefler et al., 2021; Frantar and Alistarh, 2023; Liu et al., 2023; Bansal et al., 2022), and distillation (Hinton et al., 2015; Cho and Hariharan, 2019; Tang et al., 2019; Touvron et al., 2021) have been applied to speed up the inference of the machine learning model, particularly LLMs. While these solutions are extremely effective, they often necessitate modifications to the model architecture and the training procedure. This usually involves re-training or fine-tuning the models. And it is important to note that these methods do not result in identical outputs.

Speculative Execution. Speculative execution (Burton, 1985; Hennessy and Patterson, 2011) is employed in computer architecture where a system performs some task in advance if that task is known to be required after the previous task. Speculative decoding (Chen et al., 2023; Leviathan et al., 2023) has been proposed as an effective strategy to boost the inference speed of LLMs. Previously, (Stern et al., 2018) proposed to use block-wise parallel decoding to accelerate greedy decoding of attention models. However, these methods need to train or select a high-quality draft model, and also result in increased memory overhead. Yang et al. (2023) proposed to copy the reference text tokens and validate them in a forward pass. However, this method relies on the repetitiveness assumption, and thus does not apply to general scenario generation. In contrast, our approach does not incur additional memory overhead and does not hinge on explicit assumptions about data distribution.

Early Exit. Early exit allows the model to choose different calculation paths based on the input during the inference process to achieve acceleration.

Algorithm 1 Autoregressive Decoding (Greedy)

```

1: Given model  $p(x|x_1, \dots, x_t)$ , prompt  $x_1, \dots, x_t$  and target
   sequence length  $T$ .
2: for  $i = t, \dots, T-1$  do
3:    $x_{i+1} \leftarrow \arg \max p(x|x_1, \dots, x_i)$ 
4: return  $x_1, \dots, x_T$ 

```

Various early exit techniques for encoder-only Transformers (Devlin et al., 2019) have been proposed (Xin et al., 2020b; Schwartz et al., 2020; Liu et al., 2020; Xin et al., 2020a; Hou et al., 2020; Zhou et al., 2020; Liao et al., 2021; Zhu, 2021; Li et al., 2021; Sun et al., 2022). Recently, (Schuster et al., 2022) further verified the effectiveness of early exit on the encoder-decoder LLM (Raffel et al., 2020). Inspired by these works, we opt to skip certain intermediate layers during drafting.

3 Method

In this section, we first go through the standard autoregressive decoding. Subsequently, we provide a detailed depiction of our proposed method, including selectively skipping layers during drafting, and adaptively determining the number of draft tokens.

3.1 Standard Autoregressive Decoding

Existing LLMs typically follow an autoregressive decoding process. Given a prompt sequence x_1, \dots, x_t , the model calculates the probability distribution of the next token $p(x|x_1, \dots, x_t)$. We present a greedy decoding process in Algorithm 1. In practice, instead of choosing the token with the highest probability (as in greedy decoding), we can sample tokens based on their probability distribution, which introduces some randomness and generates more diverse outputs.

Ideally, the computational cost of autoregressive decoding is comparable to that of sequence-level forward processing for an equivalent number of tokens.² However, this decoding process is significantly bounded by the memory bandwidth of the device. When decoding each token, all the model parameters need to pass through the accelerator chip. So the model size divided by the memory bandwidth gives a hard ceiling on the decoding speed, resulting in a much longer inference time.

²In fact, due to the causal nature of language modeling, autoregressive decoding could potentially save some attention computation.

Algorithm 2 Self-Speculative Decoding (Greedy)

```
1: LLM  $p(x|z^*, x_1, \dots, x_t)$  where  $x_1, \dots, x_t$  is the prompt,
    $z^*$  is a vector that represents the specific layers to bypass;
   target sequence length  $T$ ; max draft tokens to generate  $K$ .
   The  $p(x|\vec{0}, x_1, \dots, x_t)$  denotes original LLM, where  $\vec{0}$  is
   a zero vector, indicating all layers are used in inference.
2:  $i \leftarrow t$ 
3: while  $i < T$  do
4:   for  $j \leftarrow i, \dots, i + K$  do ▷ Drafting Stage
5:      $x_{j+1} \leftarrow \arg \max p(x|z^*, x_1, \dots, x_j)$ 
6:     if need to exit drafting (§3.4) then
7:       Break
8:   for  $i \leftarrow i, \dots, j$  do ▷ Verification Stage
9:     if  $x_{i+1} \neq \arg \max p(x|\vec{0}, x_1, \dots, x_i)$  then
10:       $x_{i+1} \leftarrow \arg \max p(x|\vec{0}, x_1, \dots, x_i)$ 
11:      Break
12:    $i \leftarrow i + 1$ 
13:   If all draft tokens are accepted, generate next token
    $x_{i+1} \leftarrow \arg \max p(x|\vec{0}, x_1, \dots, x_i)$  and  $i \leftarrow i + 1$ 
14: return  $x_1, \dots, x_T$ 
```

3.2 Self-Speculative Decoding

To mitigate the inherent inefficiency of autoregressive decoding, speculative decoding can be employed to enhance the inference speed of LLMs. This strategy involves two models: an LLM that we want to optimize, and a draft model that runs faster, albeit potentially at a lower quality. Speculative decoding can be explained as a two-stage process: (1) drafting: the draft model first generates K draft tokens from a given prompt sequence x_1, \dots, x_i , denoted as x_{i+1}, \dots, x_{i+K} . (2) verification: following the drafting stage, the original LLM is then employed to validate these draft tokens. This validation is accomplished in a single forward pass, where the LLM predicts the probability distributions for each draft token and assesses whether they align with the draft tokens. Once a draft token x_j is not validated, we use the original LLM’s prediction to override x_j , and start the next round of drafting beginning from token x_{j+1} .

The above process is based on the observation that computing the forward pass of a short continuation of tokens in parallel is not much slower than that of a single token. Consequently, the verification stage could be significantly more efficient than decoding tokens using the original LLM in standard autoregressive decoding.

In contrast to existing methods that use a standalone draft model to obtain draft tokens, our paper proposes a novel ‘self-speculative’ approach. We employ the original LLM itself for both the drafting and verification stages. During the drafting stage, the LLM selectively skips some of its intermediate layers so as to generate draft tokens

quicker. Subsequently, these draft tokens are verified by the original LLM. Algorithm 2 presents a detailed description of the greedy decoding process. A complete sampling-based decoding process is elaborated in Appendix K.

Despite the simplicity of the main idea of self-speculative decoding, it poses several challenges:

Challenge 1: First, it is non-trivial to determine which layers and the number of layers to skip during drafting. If an excessive number of layers are skipped, the quality of the draft could be significantly compromised. This could result in a low acceptance rate in the verification stage, consequently increasing the overall inference time. On the other hand, if fewer layers are skipped, it ensures a higher acceptance, but also caps the maximum speedup that could be achieved.

Challenge 2: It is hard to decide when to stop the generation of draft tokens. As shown in Figure 2, the choice of the number of draft tokens to generate significantly influences the end-to-end speedup. In speculative decoding, if a draft token is rejected, all subsequent draft tokens will be discarded. Therefore, generating an excessive number of draft tokens could lead to unnecessary computation, thereby increasing the inference time.

In Sections 3.3 and 3.4, we will detail our approach to address these two challenges respectively.

3.3 Selection of Skipped Layers

The selection of skipped layers is essential in our method, shaping the configuration of the draft model and, consequently, the speedup achieved via self-speculative decoding. This selection process must carefully balance two key factors: the draft model’s ‘effectiveness’ and ‘efficiency.’ Both are intrinsically linked to the selection of skipped layers and significantly influence the overall performance of our method. Specifically:

(1) The ‘effectiveness’ of the draft model is quantified by the acceptance rate, which measures the agreement between the draft and verify models. However, we note that an exclusive focus on optimizing the acceptance rate could lead to no layers being skipped, i.e. the draft model identical to the verify model, resulting in an acceptance rate of 100%, but without any speedup.

(2) On the other hand, the ‘efficiency’ of the draft model can be quantified by the number of layers in the draft model. Indeed, minimizing the number of layers can reduce the inference latency of the draft

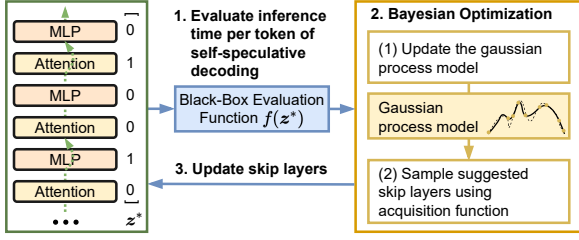


Figure 3: Illustration of using Bayesian optimization to search the best combination of skip layers that results in the lowest average token inference time.

model, but an extreme setup where all layers are skipped would result in the draft model generating low-quality tokens. This would drastically lower the acceptance rate, negating any potential speedup.

In this section, we frame the layer selection process as an optimization problem, our primary objective is to optimize the *average inference time per verified token*. This metric provides a comprehensive measure of the end-to-end inference time, including both drafting and verifying stages, normalized by the number of verified tokens.

Objective Function. This metric is a function of the selection of layers to be skipped in the draft model. The function, represented as $f(z)$, takes the selection of layers (z) as input and returns the average inference time per *verified* token on a development set. Here, z is a vector that represents the layers to be skipped.

Optimization Problem. The optimization problem’s goal is to find the input z^* that minimizes the objective function $f(z)$. This problem can be formally expressed as:

$$z^* = \arg \min_z f(z), \quad s.t. \ z \in \{0, 1\}^L. \quad (1)$$

While a brute force search could find the globally optimal solution for smaller models with a manageable solving space, it becomes prohibitively expensive for larger language models with many layers (e.g., $L = 160$ for LLaMA-2-70B).

To tackle this, we employ Bayesian optimization (Jones et al., 1998). As shown in Figure 3, it iteratively selects new inputs z^* for evaluation, based on a surrogate model of the objective function, i.e. Gaussian process (Rasmussen et al., 2006), and an acquisition function. The latter balances exploration (testing inputs where the model’s prediction is uncertain) and exploitation (testing inputs where the model anticipates a favorable result). This procedure continues until a predetermined number of iterations is reached. We use the obtained z^* to

accelerate text generation, and z^* is fixed for each model (i.e., generating draft model at model-level) without further updating. When the draft model’s target tasks vary significantly, task-level optimization is more appropriate to achieve good performance. Specifically, building the development set of optimization process from a single data source to mitigate inter-task interference.

In addition, while we here adopt skipping intermediate layers as a simple yet effective strategy to expedite the drafting stage, our scheme can be integrated with quantization (Dettmers et al., 2022) and sparsification (Sun et al., 2023) to further reduce resource consumption, as detailed in Appendix H.

3.4 Adaptive Draft-Exiting Mechanism

Our self-speculative decoding approach incorporates an adaptive draft-exiting mechanism to enhance computational efficiency during the drafting stage. In speculative decoding, if a draft token is rejected, all subsequent draft tokens will be discarded accordingly. The draft-exiting mechanism prevents the wasteful allocation of computational resources toward draft tokens that are less likely to be accepted in the verification stage.

Specifically, it compares the predicted probability of each draft token against a threshold γ . If the predicted probability falls below γ such that $p(x_{t+1}|x_1, \dots, x_t) < \gamma$, indicating low confidence, it immediately stops drafting. This approach ensures a better use of computing by focusing on the generation and verification of high-quality tokens, thereby improving the overall efficiency.

Moreover, it is worth noting that a static threshold may not accurately reflect the actual acceptance rate between the drafting and verification stages. For example, more challenging examples with a lower acceptance rate would be better served by a higher γ . To avoid the need for case-by-case threshold determination, we use an adaptive threshold that adjusts dynamically according to an updating rule, thereby allowing for an accurate reflection of the acceptance rate and better handling of examples in different difficulties. We denote the acceptance rate (AR) at e -th drafting stage as AR_e . Consequently, the update rule is defined as follows:

$$AR \leftarrow \beta_1 AR + (1 - \beta_1) AR_e, \quad (2)$$

$$\tilde{\gamma} = \begin{cases} \gamma + \epsilon, & \text{if } AR \leq \alpha \\ \gamma - \epsilon, & \text{otherwise} \end{cases}, \quad (3)$$

$$\gamma \leftarrow \beta_2 \gamma + (1 - \beta_2) \tilde{\gamma}, \quad (4)$$

where α represents a target acceptance rate, ϵ is the update step-size, and β_1 and β_2 are factors designed to mitigate fluctuations of γ and AR respectively. Notably, when e is 1, $\beta_1 = 0$. We update γ after each verification stage. This updating rule ensures that the acceptance rate remains in close proximity to a target acceptance rate α .

4 Evaluation

4.1 Setup

We evaluate a diverse range of models including LLaMA-2-13B, LLaMA-2-13B-Chat, CodeLLaMA-13B, and LLaMA-2-70B. Detailed setup can be found in Appendix B. We perform Bayesian optimization³ (BO) for 1000 iterations to select the skipped layers in the drafting stage⁴. Results of tuning the number of BO iterations are reported in Appendix E. The datasets include CNN/Daily Mail (CNN/DM), Extreme Summarization (XSum), and HumanEval. These tasks cover the evaluation of text and code generation capabilities. Appendix I shows effectiveness on more diverse tasks such as solving math problems and open-domain chitchat. We perform 1-shot evaluation for CNN/DM and XSum, and compare the ROUGE-2 (Lin, 2004). We compare pass@1 and pass@10 (Kulal et al., 2019) for HumanEval. We randomly sample 1000 instances from the testset for CNN/DM and XSum.

4.2 Main Results

We evaluate the performance of our decoding scheme, denoted as ‘Self-Speculative’, with both greedy decoding (temperature = 0.0) and random sampling (temperature = 0.2/0.6), across text and code generation. The baseline is ‘Autoregressive’, which uses the original model to perform standard autoregressive decoding. The experiments involve various scales of LLaMA-2 and its fine-tuned models. The results can be found in Tables 1 and 2. We visualize the layer skipping distribution for different models in Appendix C.

For text generation tasks, Table 1 shows that our method, when applied with temperature settings of 0.0 and 0.2 achieves considerable speedups ranging from 1.210 \times to **1.992 \times** . Another important observation from these results is the minimal to

nonexistent loss in ROUGE-2⁵, which verifies a core advantage of our decoding scheme, namely *consistent output quality*. In Appendix J.1, we compare the ROUGE-2 with other mainstream LLMs and evaluate the various metrics (ROUGE-1 and ROUGE-L) to quantitatively show our output quality. Moreover, the case study in Appendix J.2 qualitatively presents consistent output examples. In particular, our approach can be effectively applied on LLaMA-2-13B-Chat, a fine-tuned LLaMA-2-13B for conversation scenarios, indicating the compatibility of our method with fine-tuned models. This effectively addresses the dependency of the original speculative decoding method on high-quality draft models, which can be challenging to train and obtain, especially for fine-tuned models. Furthermore, the higher speedup achieved on LLaMA-2-70B suggests that larger models introduce more redundancy. This allows the drafting stage to skip a larger percentage of intermediate layers, thereby enhancing the overall speedup.

We also tested CodeLLaMA-13B, another fine-tuned LLaMA-2-13B for code generation. We used the HumanEval benchmark. Table 2 shows that we achieve speedups of 1.345 \times and 1.456 \times , respectively, while maintaining similar task scores in terms of pass@1 and pass@10. This further validates the compatibility of our scheme for coding.

4.3 Impact of Skipped Layer Selection

To investigate the impact of skipped layer selection, we conduct experiments on LLaMA-2-13B, which comprises 80 layers. Throughout the BO process, we track the number of layers skipped, denoted as $\|z^*\|$, and the speedup relative to the autoregressive baseline. Figure 4 shows the results, where the dashed line indicates the maximum speedup for runs that skip the same number of layers.

These results reveal that: (1) The peak end-to-end speedup is observed when about half of the layers are skipped during the drafting stage; (2) The specific combination of layers skipped also plays a significant role. In particular, an inappropriate combination of skipped layers can actually result in a decrease in the end-to-end inference speed. (3) There is a noticeable drop in speedup when more than 42 layers are skipped. This suggests that the quality of drafting significantly deteriorates when an excessive number of layers are omitted.

³<https://github.com/bayesian-optimization/BayesianOptimization> (MIT License) is used.

⁴Appendix B reports the offline BO time at model-level.

⁵We attribute any slight differences observed in the case of greedy decoding to numerical rounding errors.

Model	Method	Temp.	CNN/DM		XSum	
			ROUGE-2	Speedup	ROUGE-2	Speedup
LLaMA-2-13B	Autoregressive	0.0	0.106	1.000×	0.124	1.000×
LLaMA-2-13B	Self-Speculative	0.0	0.108	1.572×	0.125	1.429×
LLaMA-2-13B	Autoregressive	0.2	0.111	1.000×	0.117	1.000×
LLaMA-2-13B	Self-Speculative	0.2	0.111	1.529×	0.117	1.377×
LLaMA-2-13B-Chat	Autoregressive	0.0	0.144	1.000×	0.109	1.000×
LLaMA-2-13B-Chat	Self-Speculative	0.0	0.143	1.409×	0.109	1.224×
LLaMA-2-13B-Chat	Autoregressive	0.2	0.143	1.000×	0.106	1.000×
LLaMA-2-13B-Chat	Self-Speculative	0.2	0.145	1.383×	0.108	1.210×
LLaMA-2-70B	Autoregressive	0.0	0.130	1.000×	0.118	1.000×
LLaMA-2-70B	Self-Speculative	0.0	0.130	1.992×	0.118	1.598×
LLaMA-2-70B	Autoregressive	0.2	0.131	1.000×	0.108	1.000×
LLaMA-2-70B	Self-Speculative	0.2	0.131	1.964×	0.110	1.560×

Table 1: Evaluation on text generation tasks. ‘Speedup’ represents the acceleration of average inference time per token compared to the ‘Autoregressive’ baseline on the same setting.

Model	Method	HumanEval	Speedup
CodeLLaMA-13B	Autoreg.	pass@1	0.311
CodeLLaMA-13B	Self-Spec.	pass@1	0.317
CodeLLaMA-13B	Autoreg.	pass@10	0.659
CodeLLaMA-13B	Self-Spec.	pass@10	0.659

Table 2: Evaluation on code generation tasks. We use greedy decoding for pass@1 and random sampling with a temperature of 0.6 for pass@10.

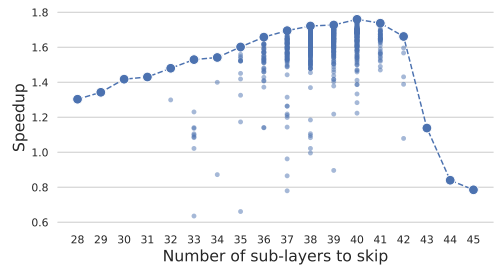


Figure 4: Speedup vs the number of skipped layers. These results are derived from the BO process.

496 These findings indicate the importance of layer
497 selection in the implementation of self-speculative
498 decoding. However, alternative layer skipping
499 strategies do not achieve satisfactory speedup com-
500 pared to BO, as detailed in Appendix D.

501 Performance degradation in drafting may be
502 compensated by adopting *aggressive skipping* strat-
503 egy and further training the draft model on a small
504 amount of data, as described in Appendix F. This
505 finding aligns with the Sheared-LLaMA (Xia et al.,
506 2023), which shows the effectiveness of pruning
507 followed by fine-tuning on a small corpus.

508 4.4 Effectiveness of Draft-Exiting

509 Here we explore the effectiveness of the adaptive
510 draft exit mechanism, specifically whether a thresh-
511 old is needed and whether a static threshold is suf-
512 ficient. Our settings are LLaMA-2-13B, CNN/DM,
513 and greedy decoding.

514 **Fixed Number of Draft Tokens.** We evaluated
515 a self-speculative decoding variant where the draft
516 model generates a constant number K of tokens.
517 As Table 3 shows, speedup initially increases with
518 K , then decreases. This pattern arises as a large K
519 (e.g., $K = 8$) produces many tokens likely to fail
520 verification, wasting computation in drafting.

521 While an appropriate K , e.g. $K = 4$, can par-
522 tially alleviate this issue, a static setting limits the

523 draft model’s potential and achieves only a modest
524 speedup (1.44×). This is because a static K does
525 not adapt to the complexity of different instances.
526 Ideally, we should use a larger K for simpler in-
527 stances and a smaller K for challenging ones.

528 Moreover, Table 3 reveals that the acceptance
529 rate and speedup do not have a direct proportion-
530 ality. For instance, when $K = 2$, the acceptance
531 rate peaks at 0.924, yet the speedup is only 1.37×.
532 This discrepancy is due to the overly conservative
533 $K = 2$, which underutilizes the draft model’s ca-
534 pacity. By generating fewer draft tokens, we miss
535 opportunities to produce more valid draft tokens,
536 thus limiting the overall speedup.

537 **Draft-Exiting with Static Threshold.** Another
538 variant is to stop generating draft tokens if the
539 confidence score falls below a predefined static
540 threshold. Table 4 shows that different static
541 thresholds have large differences in acceleration
542 (1.38×~1.58×). This highlights the importance of
543 adaptively determining the appropriate threshold
544 to optimize the speedup. Specifically, we observe
545 that high thresholds ($\gamma=0.8$) tend to underestimate
546 the capabilities of the drafting model. Despite a
547 high acceptance rate ($AR=0.935$), this does not
548 necessarily result in the best speedup due to a re-

K	2	4	6	8	Adaptive
ROUGE-2	0.107	0.107	0.107	0.107	0.108
AR	0.924	0.865	0.807	0.748	0.919
Speedup	1.37 \times	1.44 \times	1.42 \times	1.36 \times	1.57\times

Table 3: Drafting with different K values.

γ	0.2	0.4	0.6	0.8	Adaptive
ROUGE-2	0.107	0.107	0.107	0.107	0.108
AR	0.749	0.852	0.909	0.935	0.919
Speedup	1.38 \times	1.52 \times	1.58\times	1.55 \times	1.57 \times

Table 4: Static draft-exiting threshold γ with $K = 12$.

duced number of drafting tokens (1.55 \times). Conversely, a lower threshold ($\gamma=0.2$) tends to overestimate the drafting model’s capabilities, leading to a significantly lower acceptance rate ($AR=0.749$), wasting computational resources during the drafting stage, and thereby leading to slower inference speed (1.38 \times).

Draft-Exiting with Adaptive Threshold. To address the issue of optimal threshold determination, we propose an adaptive draft-exiting mechanism. Specifically, we evaluate the acceptance rate and compare it to a target acceptance rate. The threshold is updated with an updating rule depicted in Section 3.3. Table 4 shows that the speedup achieved by our adaptive threshold update method (1.57 \times) is comparable to, if not superior to, the speedup achieved with careful tuning of static thresholds. This indicates that dynamic threshold updating yields efficient and stable inference acceleration. This is mainly because the acceptance rate gets closer to the target AR by adjusting the γ value in a timely manner for instances of varying difficulties. Also, Appendix G reveals the adaptive draft-exiting is insensitive to changes in K .

4.5 Evolution of Draft-Exiting Threshold

Figure 5 captures the evolution of the draft-exiting threshold across different models and datasets over approximately 5,000 drafting and verification iterations. We can observe that our strategy adeptly adjusts the threshold, facilitating effective acceleration. However, the substantial variability across different models and datasets confirms the limitation of static threshold settings and the necessity for adaptive updates.

4.6 Breakdown of Computation

Table 5 presents a computation breakdown comparing the baseline with our ‘Self-Speculative’ decod-

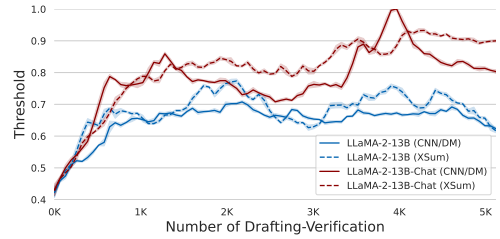


Figure 5: Threshold γ varies with models and data. We calculate a moving average for every 64 cycles and plot the standard deviation. The initial γ is set to 0.4.

Operation	Autoregressive	Self-Speculative
Drafting	-	25.5\pm1.14 ms
- Attention	-	14.6 \pm 0.65 ms
- MLP	-	9.46 \pm 0.42 ms
Verification	-	10.7 \pm 2.81 ms
- Attention	-	7.55 \pm 1.91 ms
- MLP	-	2.73 \pm 0.80 ms
γ update	-	0.61 \pm 0.14 μ s
Latency *	56.3 \pm 1.23 ms	36.8 \pm 3.23 ms
- Attention	39.7 \pm 0.91 ms	22.2 \pm 2.33 ms
- MLP	14.3 \pm 0.29 ms	12.2 \pm 1.22 ms

Table 5: Breakdown of computation. * denotes the average inference latency per token for 10 instances sampled from CNN/DM test set on LLaMA-2-13B.

ing method. Our approach exhibits a significant speedup in average inference time per token compared to ‘Autoregressive’. This speedup is primarily attributed to two key techniques: the selection of skipped layers and the adaptive draft-exiting. Notably, the drafting stage consumes the majority of inference latency, highlighting the need for draft model optimizations to improve overall inference speedup. Importantly, our adaptive exit mechanism (γ update) incurs negligible computational cost as it does not involve neural network calculations.

5 Conclusion

In this paper, we introduced self-speculative decoding, a novel and efficient inference scheme that accelerates Transformer-based LLMs. Our method does not depend on additional neural network training and incurs no extra device memory, making it a highly practical and cost-effective solution for inference acceleration. Moreover, we used Bayesian optimization to search for layers to skip in drafting and proposed an adaptive draft-exiting mechanism to improve the end-to-end inference speed. Benchmark tests with LLaMA-2 and its fine-tuned models demonstrated a speedup of up to 1.99 \times . For future work, we aim to explore more sophisticated model compression strategies to further accelerate the drafting stage for low-resource scenarios.

613	6 Ethical Considerations		
614	In compliance with ethical considerations, we emphasize that the entirety of our research revolves around open-source datasets, models, and tools. Notably, we exclusively focus on improving model inference efficiency and do not engage in any commercial usage or ethical implications.		
615			
616			
617			
618			
619			
620	7 Limitations		
621	While our self-speculative decoding scheme presents benefits for accelerating LLMs, there are a few limitations to consider. Firstly, the utilization of Bayesian optimization to determine the layers to be skipped during the drafting stage may require several hours. Nonetheless, this limitation is not critical, as this process is a one-time, offline execution at the model level. Secondly, our method does not involve any neural network training, which imposes a constraint on the number of layers that can be skipped. An excessive reduction in layers could result in a significant drop in the acceptance rate, thereby diminishing the achieved speedup. Although fine-tuning the draft model—a sub-graph of the original model—could potentially mitigate this issue and yield a better speedup, as shown in Appendix F, it incurs additional memory overhead since the draft model no longer shares the same parameters with the original model. In addition, we can refer to FlashAttention (Dao, 2023) and vLLM (Kwon et al., 2023) and similar works to further adapt our technique for batched decoding.		
622			
623			
624			
625			
626			
627			
628			
629			
630			
631			
632			
633			
634			
635			
636			
637			
638			
639			
640			
641			
642			
643	References		
644	Reza Yazdani Aminabadi, Samyam Rajbhandari, Ammar Ahmad Awan, Cheng Li, Du Li, Elton Zheng, Olatunji Ruwase, Shaden Smith, Minjia Zhang, Jeff Rasley, et al. 2022. Deepspeed-inference: Enabling efficient inference of transformer models at unprecedented scale. In <i>2022 SC22: International Conference for High Performance Computing, Networking, Storage and Analysis (SC)</i> , pages 646–660. IEEE Computer Society.		
645			
646			
647			
648			
649			
650			
651			
652			
653	Hritik Bansal, Karthik Gopalakrishnan, Saket Dingliwal, Sravan Bodapati, Katrin Kirchhoff, and Dan Roth. 2022. Rethinking the role of scale for in-context learning: An interpretability-based case study at 66 billion scale. <i>arXiv preprint arXiv:2212.09095</i> .		
654			
655			
656			
657			
658	Rishi Bommasani, Drew A Hudson, Ehsan Adeli, Russ Altman, Simran Arora, Sydney von Arx, Michael S Bernstein, Jeannette Bohg, Antoine Bosselut, Emma Brunskill, et al. 2021. On the opportunities and risks of foundation models. <i>arXiv preprint arXiv:2108.07258</i> .	662	663
659			
660			
661			
	Tom Brown, Benjamin Mann, Nick Ryder, Melanie Subbiah, Jared D Kaplan, Prafulla Dhariwal, Arvind Neelakantan, Pranav Shyam, Girish Sastry, Amanda Askell, et al. 2020. Language models are few-shot learners. <i>Advances in neural information processing systems</i> , 33:1877–1901.	664	665
		666	667
		668	669
	F Warren Burton. 1985. Speculative computation, parallelism, and functional programming. <i>IEEE Transactions on Computers</i> , 100(12):1190–1193.	670	671
		672	
	Stephanie CY Chan, Adam Santoro, Andrew Kyle Lampinen, Jane X Wang, Aaditya K Singh, Pierre Harvey Richemond, James McClelland, and Felix Hill. 2022. Data distributional properties drive emergent in-context learning in transformers. In <i>Advances in Neural Information Processing Systems</i> .	673	674
		675	676
		677	678
	Charlie Chen, Sebastian Borgeaud, Geoffrey Irving, Jean-Baptiste Lespiau, Laurent Sifre, and John Jumper. 2023. Accelerating large language model decoding with speculative sampling. <i>arXiv preprint arXiv:2302.01318</i> .	679	680
		681	682
		683	
	Jang Hyun Cho and Bharath Hariharan. 2019. On the efficacy of knowledge distillation. In <i>Proceedings of the IEEE/CVF international conference on computer vision</i> , pages 4794–4802.	684	685
		686	687
	Karl Cobbe, Vineet Kosaraju, Mohammad Bavarian, Mark Chen, Heewoo Jun, Lukasz Kaiser, Matthias Plappert, Jerry Tworek, Jacob Hilton, Reiichiro Nakano, Christopher Hesse, and John Schulman. 2021. Training verifiers to solve math word problems. <i>arXiv preprint arXiv:2110.14168</i> .	688	689
		690	691
		692	693
	Tri Dao. 2023. FlashAttention-2: Faster attention with better parallelism and work partitioning.	694	695
	Tim Dettmers, Mike Lewis, Younes Belkada, and Luke Zettlemoyer. 2022. Llm.int8(): 8-bit matrix multiplication for transformers at scale. <i>arXiv preprint arXiv:2208.07339</i> .	696	697
		698	699
	Jacob Devlin, Ming-Wei Chang, Kenton Lee, and Kristina Toutanova. 2019. BERT: pre-training of deep bidirectional transformers for language understanding. In <i>Proceedings of the 2019 Conference of the North American Chapter of the Association for Computational Linguistics: Human Language Technologies</i> .	700	701
		702	703
		704	705
		706	
	Jiarui Fang, Yang Yu, Chengduo Zhao, and Jie Zhou. 2021. Turbo Transformers: an efficient gpu serving system for transformer models. In <i>Proceedings of the 26th ACM SIGPLAN Symposium on Principles and Practice of Parallel Programming</i> , pages 389–402.	707	708
		709	710
		711	
	Elias Frantar and Dan Alistarh. 2023. Massive language models can be accurately pruned in one-shot. <i>arXiv preprint arXiv:2301.00774</i> .	712	713
		714	

715	Elias Frantar, Saleh Ashkboos, Torsten Hoefler, and Dan Alistarh. 2022. Gptq: Accurate post-training quantization for generative pre-trained transformers. <i>arXiv preprint arXiv:2210.17323</i> .	768
716		769
717		770
718		771
719	Leo Gao, Stella Biderman, Sid Black, Laurence Golding, Travis Hoppe, Charles Foster, Jason Phang, Horace He, Anish Thite, Noa Nabeshima, Shawn Presser, and Connor Leahy. 2020. The pile: An 800gb dataset of diverse text for language modeling. <i>arXiv preprint arXiv:2101.00027</i> .	772
720		773
721		774
722		
723		775
724		776
725	Song Han, Huizi Mao, and William J Dally. 2015. Deep compression: Compressing deep neural networks with pruning, trained quantization and huffman coding. <i>arXiv preprint arXiv:1510.00149</i> .	777
726		778
727		
728		779
729	Yang He, Ping Liu, Ziwei Wang, Zhilan Hu, and Yi Yang. 2019. Filter pruning via geometric median for deep convolutional neural networks acceleration. In <i>Proceedings of the IEEE/CVF conference on computer vision and pattern recognition</i> , pages 4340–4349.	780
730		781
731		782
732		783
733		
734		784
735	John L Hennessy and David A Patterson. 2011. <i>Computer architecture: a quantitative approach</i> . Elsevier.	785
736		786
737	Geoffrey Hinton, Oriol Vinyals, Jeff Dean, et al. 2015. Distilling the knowledge in a neural network. <i>arXiv preprint arXiv:1503.02531</i> , 2(7).	787
738		788
739		
740	Torsten Hoefler, Dan Alistarh, Tal Ben-Nun, Nikoli Dryden, and Alexandra Peste. 2021. Sparsity in deep learning: Pruning and growth for efficient inference and training in neural networks. <i>J. Mach. Learn. Res.</i> , 22(241):1–124.	789
741		790
742		791
743		792
744		793
745	Lu Hou, Zhiqi Huang, Lifeng Shang, Xin Jiang, Xiao Chen, and Qun Liu. 2020. Dynabert: Dynamic bert with adaptive width and depth. <i>Advances in Neural Information Processing Systems</i> , 33.	794
746		795
747		
748		796
749	HuggingFace. 2023. Text generation inference: Fast optimized inference for LLMs. https://github.com/huggingface/text-generation-inference .	797
750		798
751		799
752	Benoit Jacob, Skirmantas Kligys, Bo Chen, Menglong Zhu, Matthew Tang, Andrew Howard, Hartwig Adam, and Dmitry Kalenichenko. 2018. Quantization and training of neural networks for efficient integer-arithmetic-only inference. In <i>Proceedings of the IEEE conference on computer vision and pattern recognition</i> , pages 2704–2713.	800
753		801
754		802
755		803
756		
757		804
758		805
759	Donald R Jones, Matthias Schonlau, and William J Welch. 1998. Efficient global optimization of expensive black-box functions. <i>Journal of Global optimization</i> , 13:455–492.	806
760		807
761		808
762		809
763	Sumith Kulal, Panupong Pasupat, Kartik Chandra, Mina Lee, Oded Padon, Alex Aiken, and Percy S Liang. 2019. Spoc: Search-based pseudocode to code. <i>Advances in Neural Information Processing Systems</i> , 32.	810
764		811
765		812
766		
767		813
		814
		815
		816
		817
		818
		819
		820
		821
		768
		769
		770
		771
		772
		773
		774
		775
		776
		777
		778
		779
		780
		781
		782
		783
		784
		785
		786
		787
		788
		789
		790
		791
		792
		793
		794
		795
		796
		797
		798
		799
		800
		801
		802
		803
		804
		805
		806
		807
		808
		809
		810
		811
		812
		813
		814
		815
		816
		817
		818
		819
		820
		821

822	Markus Nagel, Mart van Baalen, Tijmen Blankevoort, and Max Welling. 2019. Data-free quantization through weight equalization and bias correction. In <i>Proceedings of the IEEE/CVF International Conference on Computer Vision</i> , pages 1325–1334.	Mitchell Stern, Noam Shazeer, and Jakob Uszkoreit. 2018. Blockwise parallel decoding for deep autoregressive models. <i>Advances in Neural Information Processing Systems</i> , 31.	877 878 879 880
827	NVIDIA. Fastertransformer. https://github.com/NVIDIA/FasterTransformer .	Mingjie Sun, Zhuang Liu, Anna Bair, and J. Zico Kolter. 2023. A simple and effective pruning approach for large language models. <i>arXiv preprint arXiv:2306.11695</i> .	881 882 883 884
829	Gunho Park, Baeseong Park, Se Jung Kwon, Byeongwook Kim, Youngjoo Lee, and Dongsoo Lee. 2022. nuqmm: Quantized matmul for efficient inference of large-scale generative language models. <i>arXiv preprint arXiv:2206.09557</i> .	Tianxiang Sun, Xiangyang Liu, Wei Zhu, Zhichao Geng, Lingling Wu, Yilong He, Yuan Ni, Guotong Xie, Xuanjing Huang, and Xipeng Qiu. 2022. A simple hash-based early exiting approach for language understanding and generation. In <i>Findings of the Association for Computational Linguistics: ACL 2022</i> .	885 886 887 888 889 890
834	Reiner Pope, Sholto Douglas, Aakanksha Chowdhery, Jacob Devlin, James Bradbury, Anselm Levskaya, Jonathan Heek, Kefan Xiao, Shivani Agrawal, and Jeff Dean. 2022. Efficiently scaling transformer inference. <i>arXiv preprint arXiv:2211.05102</i> .	Raphael Tang, Yao Lu, Linqing Liu, Lili Mou, Olga Vechtomova, and Jimmy Lin. 2019. Distilling task-specific knowledge from bert into simple neural networks. <i>arXiv preprint arXiv:1903.12136</i> .	891 892 893 894
839	Colin Raffel, Noam Shazeer, Adam Roberts, Katherine Lee, Sharan Narang, Michael Matena, Yanqi Zhou, Wei Li, and Peter J. Liu. 2020. Exploring the limits of transfer learning with a unified text-to-text transformer. <i>Journal of Machine Learning Research</i> , 21.	Hugo Touvron, Matthieu Cord, Matthijs Douze, Francisco Massa, Alexandre Sablayrolles, and Hervé Jégou. 2021. Training data-efficient image transformers & distillation through attention. In <i>International Conference on Machine Learning</i> , pages 10347–10357. PMLR.	895 896 897 898 899 900
844	Carl Edward Rasmussen, Christopher K Williams, et al. 2006. Gaussian processes for machine learning, vol. 1.	Hugo Touvron, Louis Martin, Kevin Stone, Peter Albert, Amjad Almahairi, Yasmine Babaei, Nikolay Bashlykov, Soumya Batra, Prajjwal Bhargava, Shrutu Bhosale, et al. 2023. Llama 2: Open foundation and fine-tuned chat models. <i>arXiv preprint arXiv:2307.09288</i> .	901 902 903 904 905 906
847	Baptiste Rozière, Jonas Gehring, Fabian Gloeckle, Sten Sootla, Itai Gat, Xiaoqing Ellen Tan, Yossi Adi, Jingyu Liu, Tal Remez, Jérémy Rapin, Artyom Kozhevnikov, I. Evtimov, Joanna Bitton, Manish P Bhatt, Cristian Canton Ferrer, Aaron Grattafiori, Wenhan Xiong, Alexandre D’efossez, Jade Copet, Faisal Azhar, Hugo Touvron, Louis Martin, Nicolas Usunier, Thomas Scialom, and Gabriel Synnaeve. 2023. Code llama: Open foundation models for code. <i>arXiv preprint arXiv:2308.12950</i> .	Xiaohui Wang, Ying Xiong, Yang Wei, Mingxuan Wang, and Lei Li. 2021. Lightseq: A high performance inference library for transformers. In <i>Proceedings of the 2021 Conference of the North American Chapter of the Association for Computational Linguistics: Human Language Technologies: Industry Papers</i> , pages 113–120.	907 908 909 910 911 912 913
857	Tal Schuster, Adam Fisch, Jai Gupta, Mostafa Dehghani, Dara Bahri, Vinh Tran, Yi Tay, and Donald Metzler. 2022. Confident adaptive language modeling. <i>Advances in Neural Information Processing Systems</i> , 35.	Mengzhou Xia, Tianyu Gao, Zhiyuan Zeng, and Danqi Chen. 2023. Sheared LLaMA: Accelerating language model pre-training via structured pruning .	914 915 916
862	Roy Schwartz, Gabriel Stanovsky, Swabha Swayamdipta, Jesse Dodge, and Noah A. Smith. 2020. The right tool for the job: Matching model and instance complexities. In <i>Proceedings of the 58th Annual Meeting of the Association for Computational Linguistics</i> .	Guangxuan Xiao, Ji Lin, Mickael Seznec, Julien Demouth, and Song Han. 2022. Smoothquant: Accurate and efficient post-training quantization for large language models. <i>arXiv preprint arXiv:2211.10438</i> .	917 918 919 920
868	Noam Shazeer. 2019. Fast transformer decoding: One write-head is all you need. <i>arXiv preprint arXiv:1911.02150</i> .	Ji Xin, Rodrigo Nogueira, Yaoliang Yu, and Jimmy Lin. 2020a. Early exiting BERT for efficient document ranking. In <i>Proceedings of SustaiNLP: Workshop on Simple and Efficient Natural Language Processing</i> .	921 922 923 924
871	Ying Sheng, Lianmin Zheng, Binhang Yuan, Zhuohan Li, Max Ryabinin, Daniel Y Fu, Zhiqiang Xie, Beidi Chen, Clark Barrett, Joseph E Gonzalez, et al. 2023. High-throughput generative inference of large language models with a single gpu. <i>arXiv preprint arXiv:2303.06865</i> .	Ji Xin, Raphael Tang, Jaejun Lee, Yaoliang Yu, and Jimmy Lin. 2020b. DeeBERT: Dynamic early exiting for accelerating BERT inference. In <i>Proceedings of the 58th Annual Meeting of the Association for Computational Linguistics</i> .	925 926 927 928 929

Nan Yang, Tao Ge, Liang Wang, Binxing Jiao, Daxin Jiang, Linjun Yang, Rangan Majumder, and Furu Wei. 2023. Inference with reference: Lossless acceleration of large language models. *arXiv preprint arXiv:2304.04487*.

Zhewei Yao, Reza Yazdani Aminabadi, Minjia Zhang, Xiaoxia Wu, Conglong Li, and Yuxiong He. 2022. Zeroquant: Efficient and affordable post-training quantization for large-scale transformers. *arXiv preprint arXiv:2206.01861*.

Gyeong-In Yu, Joo Seong Jeong, Geon-Woo Kim, Soojeong Kim, and Byung-Gon Chun. 2022. Orca: A distributed serving system for {Transformer-Based} generative models. In *16th USENIX Symposium on Operating Systems Design and Implementation (OSDI 22)*, pages 521–538.

Ritchie Zhao, Yuwei Hu, Jordan Dotzel, Chris De Sa, and Zhiru Zhang. 2019. Improving neural network quantization without retraining using outlier channel splitting. In *International conference on machine learning*, pages 7543–7552. PMLR.

Lianmin Zheng, Wei-Lin Chiang, Ying Sheng, Siyuan Zhuang, Zhanghao Wu, Yonghao Zhuang, Zi Lin, Zhuohan Li, Dacheng Li, Eric. P Xing, Hao Zhang, Joseph E. Gonzalez, and Ion Stoica. 2023. [Judging llm-as-a-judge with mt-bench and chatbot arena](#).

Wangchunshu Zhou, Canwen Xu, Tao Ge, Julian McAuley, Ke Xu, and Furu Wei. 2020. Bert loses patience: Fast and robust inference with early exit. *Advances in Neural Information Processing Systems*, 33.

Wei Zhu. 2021. Leebert: Learned early exit for bert with cross-level optimization. In *Proceedings of the 59th Annual Meeting of the Association for Computational Linguistics*.

A Data

The datasets that we have selected for evaluation are CNN/Daily Mail (CNN/DM), Extreme Summarization (XSum), and HumanEval. These tasks cover a broad spectrum of language processing capabilities, including text and code generation capabilities. We perform 1-shot evaluation for CNN/DM and XSum, and compare the ROUGE-2. We compare pass@10 for HumanEval. For the results of efficiency, we randomly sample 1000 instances from the testset for CNN/DM and XSum.

CNN/Daily Mail (CNN/DM): This task involves summarizing news articles from the CNN and Daily Mail websites. The models are required to generate a concise summary of each article, testing their ability to understand and condense complex information.

Extreme Summarization (XSum): In the XSum task, models are asked to produce a single-sentence summary of a news article. This task tests the models’ capability to extract the most salient information from a text and express it in a single, coherent sentence.

HumanEval: The HumanEval task is a benchmark for Python programming. This task challenges the models with a variety of coding problems that require a wide range of skills, from basic programming to complex problem-solving abilities. It serves to evaluate the models’ understanding of Python syntax, their ability to implement algorithms, and their proficiency in problem-solving using code. This benchmark provides a unique perspective on the models’ capabilities in the realm of programming, complementing the language-focused tasks.

B Setup

We present the hyperparameter settings of the experiments in Table 6, including the parameters involved in the decoding process, the adaptive draft-exiting mechanism, and the random sampling. For the adaptive draft-exiting mechanism, we set the initial threshold $\gamma = 0.6$, $\epsilon = 0.01$, $\beta_1 = 0.5$, $\beta_2 = 0.9$, and α is slightly tuned for the data and model, as detailed in Table 6. For sampling-based inference, we by default use $top_p = 0.85$ for text summarization tasks, and 0.95 for code generation tasks.

In addition, the key experimental environments on the A100-40GB are CUDA 11.6, PyTorch 1.13.1, and Transformer 4.33.1; For the A100-80GB, the environment is CUDA 11.8, PyTorch 2.0.1, and Transformer 4.33.1. We use an A100-40GB to conduct experiments for LLaMA-2-13B, LLaMA-2-13B-Chat, and CodeLLaMA-13B. We use two A100-80GB with HuggingFace’s accelerate⁶ to conduct experiments for LLaMA-2-70B.

We randomly select 8 instances from the train set and use them to evaluate the inference time per token for Bayesian optimization. This randomness not only ensures the generalizability of our approach but also mitigates any potential bias that could be introduced by the data selection process. The offline Bayesian optimization time for 1000 iterations is about 2.5 hours for LLaMA-2-13B,

⁶<https://github.com/huggingface/accelerate> (Apache-2.0 License)

LLaMA-2-13B-Chat, and CodeLLaMA-13B, and about 6 hours for LLaMA-2-70B.

C Which layers are skipped?

Figure 6 visualizes the distinct base models corresponding to layer skip distributions within the draft model. Two key observations are made as follows:

First, we observe that there are more skips in the attention layer compared to the MLP layer, suggesting the attention layer is more effective for reducing inference time. This is reinforced by the results in Table 5, where the time spent in the attention layer significantly contributes to the average inference latency per token.

Second, regardless of whether it is the MLP layer or the attention layer, the skipped layers tend to cluster in the latter half of the model. This pattern suggests that most tokens can be accurately predicted in the first half of the model, leaving the second half of the model relatively redundant.

D Effect of Skip Strategy

Here, we explore the effect of various skip strategies on the performance of generated draft models. We evaluate the CNN/DM on LLaMA-2-13B. Initially, we determine the number of skipped layers using Bayesian optimization, as illustrated in Figure 6(a). We find that the attention layer skips 24 layers, while the MLP layer skips 12 layers. We proceed to apply four strategies, each involving an equal number of layer skips: skipping the initial layers ("First"), middle layers ("Mid."), final layers ("Last"), and randomly sampling layers ("Rand."). The layer skip distribution is visualized in Figure 7.

Table 7 reveals that the fixed strategies of layer skip (first, middle, last) or random skip yield minimal acceleration compared to Bayesian optimization (BO) results. These suboptimal strategies, not optimized for average inference time, result in a draft model with subpar performance (manifested as very low AR), inefficient resource utilization in the drafting phase, and ultimately, a lack of speedup. Furthermore, a slightly enhanced speedup is observed when skipping the last layers, likely due to the more severe redundancy in the model's final portion.

E Number of Iterations of BO

Subsequently, we explore the influence of the iteration number of Bayesian optimization on the performance of our decoding scheme and report

the results in Table 8. The layer skip distribution corresponding to different iteration numbers is depicted in Figure 8.

When applied to the LLaMA-2-13B for the CNN/DM task, we observe that while a higher number of iterations can yield increased acceleration, even a relatively modest number of iterations (e.g., 200) effectively reduces inference time, achieving a speedup of $1.35\times$. Notably, the performance metrics for the 800 and 1000 iterations exhibit consistency due to the same layers being skipped, as shown in Figure 8.

F Aggressive Skip

In pursuit of higher inference acceleration for users with ample resources, we explore a more aggressive skip strategy to obtain the draft model. To mitigate the performance degradation associated with the aggressive skip, we further train the draft model using 50,000 instances from the Pile dataset (Gao et al., 2020), truncating the length of each to 512 tokens, which total up to 25 million tokens. We repeat this training for 3 epochs, resulting in a cumulative utilization of 75 million tokens.

The implementation of the aggressive skip involves skipping the top-K layers based on Bayesian optimization probabilities. For instance, in the case of LLaMA-2-13B, as illustrated in Figure 9, we opt to skip 75% of the attention layers (30 layers) and 32.5% of the MLP layers (13 layers).

Table 9 reveals that when we employ a more aggressive skip without further training (#token is 0), there is a noticeable decrease in the draft model's quality, with an average acceptance rate of only 0.695. This leads to a significantly reduced speedup of merely $1.15\times$. Nevertheless, by dedicating a portion of the corpus to training, we notably enhance the draft model's quality, increasing the AR to 0.900, in line with the target acceptance rate of 0.90. This enhancement enables a further improvement in speedup from $1.57\times$ (shown in Table 1) to $1.96\times$ (trained for 60M tokens), as more layers are skipped⁷. After training on 75 million tokens, the reason for the reduced acceleration is that we believe the model has a certain degree of overfitting. It is essential to highlight that the aggressive skip strategy necessitates both an extended training process and the additional storage of trained

⁷This finding aligns with the recent Sheared-LLaMA (Xia et al., 2023), which shows the effectiveness of pruning followed by further training on a small amount of data.

Data	Model	Decoding		Adaptive Draft-Exiting					Random Sampling	
		T	K	α	ϵ	β_1	β_2	γ_0	top_p	temperature
CNN/DM	LLaMA-2-13B	512	12	0.90	0.01	0.50	0.90	0.60	0.85	0.20
CNN/DM	LLaMA-2-13B-Chat	512	12	0.85	0.01	0.50	0.90	0.60	0.85	0.20
CNN/DM	LLaMA-2-70B	512	12	0.85	0.01	0.50	0.90	0.60	0.85	0.20
XSum	LLaMA-2-13B	512	12	0.85	0.01	0.50	0.90	0.60	0.85	0.20
XSum	LLaMA-2-13B-Chat	512	12	0.70	0.01	0.50	0.90	0.60	0.85	0.20
XSum	LLaMA-2-70B	512	12	0.85	0.01	0.50	0.90	0.60	0.85	0.20
HumanEval	CodeLLaMA-13B	512	12	0.90	0.01	0.50	0.90	0.60	0.95	0.60
GSM8K	CodeLLaMA-13B	512	12	0.90	0.01	0.50	0.90	0.60	0.95	0.60
GSM8K	CodeLLaMA-13B-Instruct	512	12	0.80	0.01	0.50	0.90	0.60	0.95	0.60
MT-bench	LLaMA-2-13B-Chat	512	12	0.85	0.01	0.50	0.90	0.60	0.85	0.20

Table 6: Hyperparameter settings. γ_0 represents the default initial value of γ .

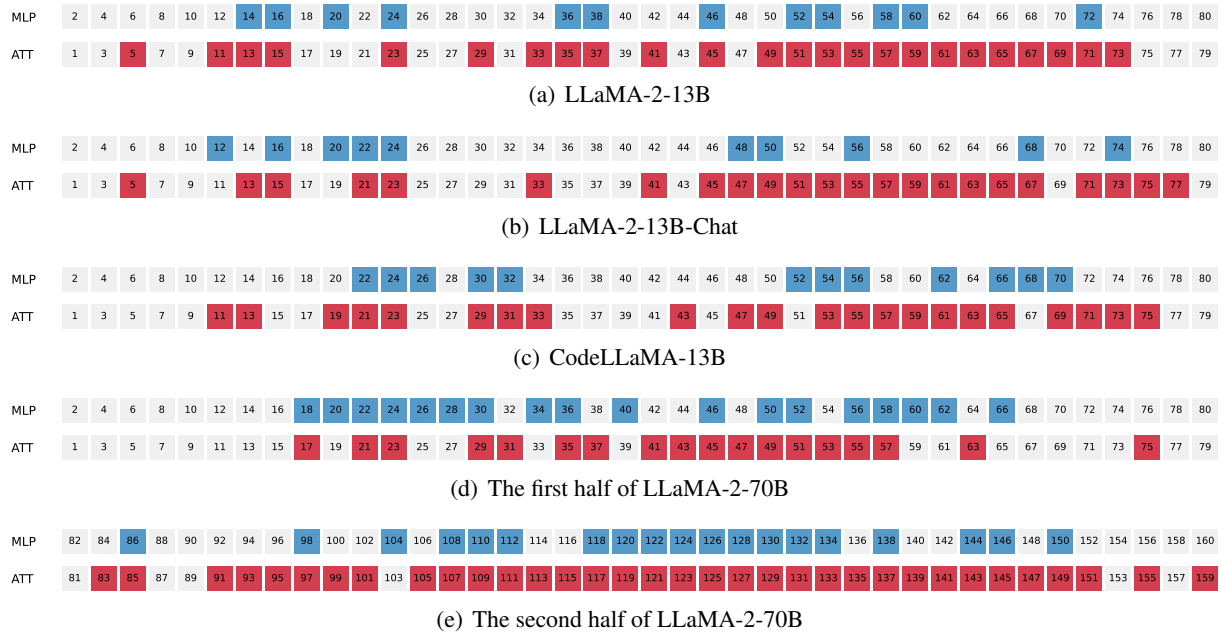


Figure 6: Visualization of layer skip distributions in draft models for various base models. Gray squares indicate retained layers, red squares denote skipped attention layers, and blue squares signify skipped MLP layers.

Strategy	First	Mid.	Last	Rand.	BO
ROUGE-2	0.108	0.108	0.107	0.107	0.108
AR	0.091	0.393	0.508	0.592	0.919
Speedup	0.696×	0.887×	0.951×	1.01×	1.57×

Table 7: The effects of different skip strategies on the performance of CNN/DM on LLaMA-2-13B.

#Iteration	200	400	600	800	1000
ROUGE-2	0.108	0.107	0.108	0.108	0.108
AR	0.903	0.938	0.920	0.919	0.919
Speedup	1.35×	1.52×	1.58×	1.57×	1.57×

Table 8: The effect of the number of iterations of Bayesian optimization.

#Token	0	20M	40M	60M	75M
ROUGE-2	0.106	0.106	0.106	0.106	0.106
AR	0.695	0.902	0.901	0.900	0.893
Speedup	1.15×	1.91×	1.94×	1.96×	1.85×

Table 9: The effect of the number of tokens on aggressive skip performance.

K	10	12	14	16	18
ROUGE-2	0.107	0.108	0.108	0.108	0.107
AR	0.924	0.919	0.916	0.913	0.911
Speedup	1.57×	1.57×	1.58×	1.58×	1.58×

Table 10: The effect of the max draft token under the adaptive draft-exiting mechanism.

G Effect of Max # of Draft Tokens

1126

draft models. However, this trade-off is deemed acceptable for users with rich resources.

Ideally, increasing the maximum number of draft tokens K while maintaining a high acceptance rate

1127

1128

Quantization	bf16	fp8	fp4	nf4
ROUGE-2 \uparrow	0.107	0.105	0.101	0.114
AR \uparrow	0.910	0.911	0.913	0.910
VRAM (GB) \downarrow	37.2	27.5	19.6	19.7
Latency (ms) \downarrow	32.4	113	152	126
Speedup \uparrow	1.53 \times	1.61\times	1.36 \times	1.35 \times

Table 11: Performance of self-speculative decoding combined with different quantization schemes of LLM.int8().

should lead to further improvements in inference acceleration. To explore this, we test the CNN/DM task using LLaMA-2-13B, varying the max draft token K , and present the results in Table 10. It is noteworthy that as K increases, the speedup remains relatively stable. This observation is primarily attributed to the fact that most tokens do not benefit from excessively large K and tend to exit early. In summary, our inference approach shows *insensitivity* to K thanks to the adaptive draft-exiting mechanism. Moreover, setting a relatively large value for K (our default is 12) allows this mechanism to perform optimally.

H Adaptation

We here adopt skipping intermediate layers as a simple yet effective strategy to expedite the drafting stage. While other acceleration techniques such as quantization and structured pruning exist, they fail to offer speed-up proportional to their compression ratio. Meanwhile, they require a separate copy of the altered model parameters, thereby increasing memory overhead. This contradicts the key requirement of no extra memory. Consequently, we adopt layer skipping in our approach. However, our scheme can be integrated with quantization (Dettmers et al., 2022) and sparsification (Sun et al., 2023) to further reduce resource consumption. In this section, we explore the combination of self-speculative decoding with quantization and sparsification techniques to adapt to users with limited computing resources. We conduct experiments on the CNN/DM task using LLaMA-2-13B, and the layer skip distribution corresponding to the draft model is shown in Figure 10.

H.1 Quantization

First, we integrate our inference approach with the quantization technique, LLM.int8()⁸ (Dettmers et al., 2022). We evaluate the performance of three

⁸<https://github.com/TimDettmers/bitsandbytes> (MIT License)

Sparsification	dense	unstructured	4:8	2:4
ROUGE-2 \uparrow	0.107	0.114	0.115	0.110
AR \uparrow	0.910	0.918	0.912	0.911
VRAM (GB) \downarrow	37.2	35.9	35.9	35.9
Latency (ms) \downarrow	32.4	30.4	29.2	30.9
Speedup \uparrow	1.57\times	1.50 \times	1.47 \times	1.48 \times

Table 12: Performance of self-speculative decoding combined with different sparsification schemes of wanda.

quantization schemes: fp8 (8-bit floating-point), fp4 (4-bit floating-point), and nf4 (4-bit normalized float), in comparison to the default bf16 (16-bit brain float point). The results are presented in Table 11. In all quantization settings, we skip the ‘lm head’ layer of the model and do not employ double quantization to save an additional 0.4 bits.

Table 11 illustrates that all three quantization schemes effectively reduce the video memory demand during inference. Notably, the fp4 quantization results in up to a nearly two-fold reduction in memory demand to just 19.6 GB. While there may be an increase in the average inference latency per token due to the dequantization process, this approach makes LLM suitable for scenarios with limited device memory.

H.2 Sparsification

Subsequently, we assess the performance of self-speculative decoding combined with sparsification techniques, specifically wanda⁹ (Sun et al., 2023), which includes unstructured sparsity and structured N:M sparsity (4:8 and 2:4) with the sparsity ratio of 0.5. The N:M sparsity constraint specifies that no more than N out of every M contiguous weights can be non-zero.

Table 12 shows that while sparsification may not dramatically reduce VRAM requirements, it does result in a reduction in the average inference latency per token to varying degrees. However, the speedup is slightly down because the base model is also accelerated.

I Exploration of Diverse Tasks

We want to mention that our approach does not require model fine-tuning and its lossless characteristic is task-agnostic. However, we are open to evaluating the effectiveness of our approach on more diverse tasks. Here, we further explore the performance of our decoding scheme on solving

⁹<https://github.com/locuslab/wanda> (MIT License)

Data	Model	Method	Perfor.	Speedup
GSM8K	CodeLLaMA-13B	Autoreg.	0.104	1.000×
GSM8K	CodeLLaMA-13B	Self-Spec.	0.101	1.351×
GSM8K	CodeLLaMA-13B-Ins.	Autoreg.	0.223	1.000×
GSM8K	CodeLLaMA-13B-Ins.	Self-Spec.	0.213	1.263×
MT-bench	LLaMA-2-13B-Chat	Autoreg.	6.940	1.000×
MT-bench	LLaMA-2-13B-Chat	Self-Spec.	6.930	1.269×

Table 13: Evaluation on solving math problem and open-domain chitchat tasks. We use greedy decoding for the accuracy of GSM8K. We use random sampling for the average score at task-level of the MT-bench with various temperatures of 0.7 for ‘writing’ and ‘roleplay’, 0.1 for ‘stem’ and ‘humanities’, and greedy decoding for the rest of the tasks, according to (Zheng et al., 2023).

1205 math problems (Grade School Math 8K (Cobbe
1206 et al., 2021)) and open-domain chitchat (MT-bench
1207 (Zheng et al., 2023)). For GSM8K, we evaluate on
1208 base model CodeLLaMA-13B and CodeLLaMA-
1209 13B-Instruct and report the problem-solving accu-
1210 racy of 1318 questions in the test set. For MT-
1211 bench, our base model is LLaMA-2-13B-Chat, and
1212 we use its program script to ask GPT-4 to give a
1213 score of 10 points for each round using their prompt
1214 templates and report the average score for a total
1215 of 160 answers for two turns of 80 questions.

1216 **Grade School Math 8K (GSM8K):** A dataset
1217 of 8.5K high-quality linguistically diverse grade
1218 school math word problems. The dataset was cre-
1219 ated to support the task of question answering on
1220 basic mathematical problems that require multi-
1221 step reasoning. Solutions primarily involve per-
1222 forming a sequence of elementary calculations us-
1223 ing basic arithmetic operations (+-×÷) to reach the
1224 final answer. This task is generally used to test
1225 logic and math in language modeling.

1226 **MT-bench:** A benchmark consisting of 80 high-
1227 quality multi-turn questions. MT-bench is designed
1228 to test multi-turn conversation and instruction-
1229 following ability, covering common use cases and
1230 focusing on challenging questions to differentiate
1231 models. The tasks identify 8 common categories
1232 of user prompts to guide its construction: writ-
1233 ing, roleplay, extraction, reasoning, math, coding,
1234 knowledge I (STEM), and knowledge II (human-
1235 ities/social science). For each category, The task
1236 manually designed 10 multi-turn questions.

1237 Regarding using Bayesian optimization 1,000
1238 iterations to generate a draft model, for GSM8K,
1239 we randomly sampled 4 samples from the training
1240 set as a development set; for MT-bench, we let
1241 GPT-3.5 generate 8 examples according to 8 topics

Model	CNN/DM	XSum
LLaMA-2-13B (ours)	0.106	0.124
LLaMA-2-13B-Chat (ours)	0.144	0.109
LLaMA-2-70B (ours)	0.130	0.118
OPT (66B)	0.136	0.126
Davinci (175B)	0.127	0.126
Palmyra X (43B)	0.049	0.149
GPT-NeoX (20B)	0.123	0.102
Luminous Base (13B)	0.110	0.105
BLOOM (176B)	0.080	0.030
YaLM (100B)	0.017	0.021

Table 14: Our model with self-speculative decoding vs. Mainstream LLMs with autoregressive.

Model	Method	ROUGE			Speedup
		1	2	L	
CNN/DM	Autoreg.	0.263	0.106	0.181	1.000×
CNN/DM	Self-Spec.	0.266	0.108	0.183	1.429×
XSum	Autoreg.	0.327	0.124	0.260	1.000×
XSum	Self-Spec.	0.328	0.125	0.261	1.377×

Table 15: Evaluation on text generation tasks with various metrics and greedy decoding.

1242 to form an optimized use development set. Other
1243 relevant hyperparameters are shown in Table 6.

1244 For GSM8K, we achieve a 1.35× acceleration
1245 without compromising task performance. Regard-
1246 ing MT-bench, spanning writing, roleplay, reason-
1247 ing, math, coding, extraction, stem, and human-
1248 ities, presents substantial task diversity, posing
1249 challenges for generating high-quality and diverse
1250 output from draft models. Nevertheless, we still
1251 achieve a speedup of about 1.27× with lossless
1252 task performance. These findings demonstrate the
1253 robustness and commendable performance of our
1254 approach across diverse tasks.

1255 J Exploration of Output Quality

1256 J.1 Quantitative Analysis

1257 **LLMs Comparison.** Considering this non-fine-
1258 tuned, one-shot setting, our score is indeed quite
1259 competitive. We attach in Table 14 the perfor-
1260 mance of other mainstream large language models
1261 on CNN/DM and XSum as a reference (data from
1262 HELM leaderboard (Liang et al., 2022)).

1263 **Diverse Metrics.** Our experimental setup mainly
1264 follows the work of DeepMind (Chen et al., 2023).
1265 For summarization tasks, ROUGE-2 is a widely
1266 recognized evaluation metric, as adopted by (Chen
1267 et al., 2023; Liang et al., 2022), in addition to
1268 ROUGE-1 and ROUGE-L. However, we want to
1269 emphasize that we have not disregarded the im-
1270 portance of other metrics such as ROUGE-1 and

ROUGE-L. Indeed, we have maintained records of these results as part of our comprehensive analysis, and we will attach them in the appendix in the revision. The results are presented below. And we can see that our conclusions remain consistent – we have been successful in achieving a significant acceleration in task performance without compromising the quality of the outputs. We believe this reaffirms the robustness and efficacy of our approach.

J.2 Qualitative Analysis

We present more qualitative evidence to supplement the quantitative ROUGE-2 score. Please note, however, that our approach is inherently lossless and the performance evaluation is conducted on the original model without any fine-tuning. The task performance of our self-speculative decoding is therefore reliant on the inherent capabilities of the base model utilizing autoregressive decoding. Specifically, using the same base model, in the greedy setting, generation results from self-speculative decoding are **identical** to those of autoregressive decoding; In the sampling setting, the results generated are from the same distribution as those for autoregressive decoding. These properties of speculative decoding have been mathematically proven in previous work (Leviathan et al., 2023). Finally, to address concerns, we present a case study on LLaMA-2-13B, detailed in the Table 16.

K Algorithm with Sampling

We first demonstrate self-speculative sampling with greedy sampling by integrating the adaptive draft-exiting mechanism in Algorithm 3.

In addition to the greedy version of self-speculative decoding that we have presented in the main paper, we also explore a variant that incorporates random sampling, that also incorporated a complete adaptive draft-exiting mechanism, as shown in Algorithm 4. This approach introduces an element of randomness into the selection of tokens for speculative decoding, as opposed to the deterministic nature of the greedy version. In our setup, random sampling is affected by two parameters: temperature and top_p . Higher values of temperature or top_p lead to greater token diversity, while lower values make token selection more deterministic. This variant could potentially lead to diverse decoding paths and outcomes, which may be beneficial in certain scenarios, such as code generation.

Algorithm 3 Self-Speculative Decoding (Greedy)

```

1: LLM  $p(x|z^*, x_1, \dots, x_t)$  where  $x_1, \dots, x_t$  is the prompt,
 $z^*$  is a vector that represents the specific layers to bypass;
target sequence length  $T$ ; max draft tokens to generate
 $K$ . We denote the original LLM as  $p(x|\vec{0}, x_1, \dots, x_t)$ ,
where  $\vec{0}$  is a zero vector, indicating all layers are used in
inference. We denote the acceptance rate ( $AR$ ) at  $e$ -th
drafting stage as  $AR_e$ .
2:  $i \leftarrow t$ 
3: while  $i < T$  do
4:   for  $j \leftarrow i, \dots, i + K$  do ▷ Drafting Stage
5:      $x_{j+1} \leftarrow \arg \max p(x|z^*, x_1, \dots, x_j)$ 
6:     if  $\max p(x|z^*, x_1, \dots, x_j) < \gamma$  then ▷ Draft Exit
7:       Break
8:   for  $i \leftarrow i, \dots, j$  do ▷ Verification Stage
9:     if  $x_{i+1} \neq \arg \max p(x|\vec{0}, x_1, \dots, x_i)$  then
10:       $x_{i+1} \leftarrow \arg \max p(x|\vec{0}, x_1, \dots, x_i)$ 
11:      Break
12:    $i \leftarrow i + 1$ 
13:   If all draft tokens are accepted, generate next token
 $x_{i+1} \leftarrow \arg \max p(x|\vec{0}, x_1, \dots, x_i)$  and  $i \leftarrow i + 1$ 
14:    $AR \leftarrow \beta_1 AR + (1 - \beta_1) AR_e$  ▷  $\gamma$  Update
15:   if  $AR \leq \alpha$  then
16:      $\gamma + \epsilon$ 
17:   else
18:      $\gamma - \epsilon$ 
 $\gamma \leftarrow \beta_2 \gamma + (1 - \beta_2) \tilde{\gamma}$ 
19: return  $x_1, \dots, x_T$ 

```

Data	Temp.	Article/Document	Summary/Highlight		
			Reference	Autoregressive	Self-Speculative
CNN/DM	0.0	An Arkansas woman became a little richer this week after finding a large diamond at Crater of Diamonds State Park. Susie Clark, of Evening Shade, found the 3.69-carat white diamond in a 37.5-acre search field on Thursday, her last day of a trip to the park with her husband. Clark,	Susie Clark, of Evening Shade, Arkansas, found the diamond on Thursday at Crater of Diamonds State Park . The 3.69-carat gem is teardrop-shaped about the size of a pinto bean . Park interpreter said it's the largest of the 122 diamonds found this year .	woman who found a 3.69-carat white diamond at Crater of Diamonds State Park in Arkansas has named the gem a 'hallelujah diamond' because she spotted the gem shortly after praying that she would find something .	woman who found a 3.69-carat white diamond at Crater of Diamonds State Park in Arkansas has named the gem a 'hallelujah diamond' because she spotted the gem shortly after praying that she would find something .
CNN/DM	0.2	who first visited the park 33 years ago with her mother and grandmother, prayed to God, asking, 'Are you doing to bless me and let me find a diamond today?' as she searched the field. Susie Clark, of Evening Shade, Arkansas, found a 3.69-carat white ...	Susie Clark, of Evening Shade, Arkansas, found the diamond on Thursday at Crater of Diamonds State Park . The 3.69-carat gem is teardrop-shaped about the size of a pinto bean . Park interpreter said it's the largest of the 122 diamonds found this year .	woman who found a 3.69-carat diamond at Crater of Diamonds State Park in Arkansas has named the gem a 'hallelujah diamond' because she spotted the gem shortly after praying that she would find something .	woman who found a 3.69-carat white diamond at Crater of Diamonds State Park in Arkansas has named the gem a 'hallelujah diamond' because she spotted the gem shortly after praying that she would find something .
XSum	0.0	The flight provider operates a "bug bounty" scheme that rewards hackers for privately disclosing security flaws rather than sharing them online. It has given the maximum reward of a million flight miles, worth dozens of trips, to two people. One security expert said the ...	US airline United has rewarded two hackers who spotted security holes in its website with a million free flight miles each.	Airlines has given out its first rewards to hackers who reported security flaws in its website.	Airlines has given out its first rewards to hackers who reported security flaws in its website.
XSum	0.2	online. It has given the maximum reward of a million flight miles, worth dozens of trips, to two people. One security expert said the ...	US airline United has rewarded two hackers who spotted security holes in its website with a million free flight miles each.	airline has given out two million flight miles to hackers who found security flaws in its website.	airline has given the maximum reward of a million flight miles, worth dozens of trips, to two people.

Table 16: Case study of CNN/DM and XSum on LLaMA-2-13B.

Algorithm 4 Self-Speculative Decoding

```

1: LLM  $p(x|\mathbf{z}^*, x_1, \dots, x_t)$  where  $x_1, \dots, x_t$  is the prompt,  $\mathbf{z}^*$  is a vector that represents the specific layers to bypass; target
   sequence length  $T$ ; max draft tokens to generate  $K$ . We denote the original LLM as  $p(x|\vec{0}, x_1, \dots, x_t)$ , where  $\vec{0}$  is a zero
   vector, indicating all layers are used in inference. We denote the acceptance rate ( $AR$ ) at  $e$ -th drafting stage as  $AR_e$ .
2:  $i \leftarrow t$ 
3: while  $i < T$  do
4:   for  $j \leftarrow i, \dots, i + K$  do ▷ Drafting Stage
5:      $x_{j+1} \leftarrow \text{sample } p(x|\mathbf{z}^*, x_1, \dots, x_j)$ 
6:     if  $\max p(x|\mathbf{z}^*, x_1, \dots, x_j) < \gamma$  then ▷ Draft Exiting
7:       Break
8:   for  $i \leftarrow i, \dots, j$  do ▷ Verification Stage
9:      $r \leftarrow \text{sample from a uniform distribution } U[0, 1]$ 
10:    if  $r \geq \min(1, \frac{p(x|\vec{0}, x_1, \dots, x_i)}{p(x|\mathbf{z}^*, x_1, \dots, x_i)})$  then
11:       $x_{i+1} \leftarrow \text{sample from } \frac{\max(0, p(x|\vec{0}, x_1, \dots, x_i) - p(x|\mathbf{z}^*, x_1, \dots, x_i))}{\sum_x \max(0, p(x|\vec{0}, x_1, \dots, x_i) - p(x|\mathbf{z}^*, x_1, \dots, x_i))}$ 
12:      Break
13:     $i \leftarrow i + 1$ 
14:    If all draft tokens are accepted, generate next token  $x_{i+1} \leftarrow \text{sample } p(x|\vec{0}, x_1, \dots, x_i)$  and  $i \leftarrow i + 1$ 
15:     $AR \leftarrow \beta_1 AR + (1 - \beta_1) AR_e$  ▷  $\gamma$  Updating
16:    if  $AR \leq \alpha$  then
17:       $\gamma + \epsilon$ 
18:    else
19:       $\gamma - \epsilon$ 
       $\gamma \leftarrow \beta_2 \gamma + (1 - \beta_2) \tilde{\gamma}$ 
20: return  $x_1, \dots, x_T$ 

```

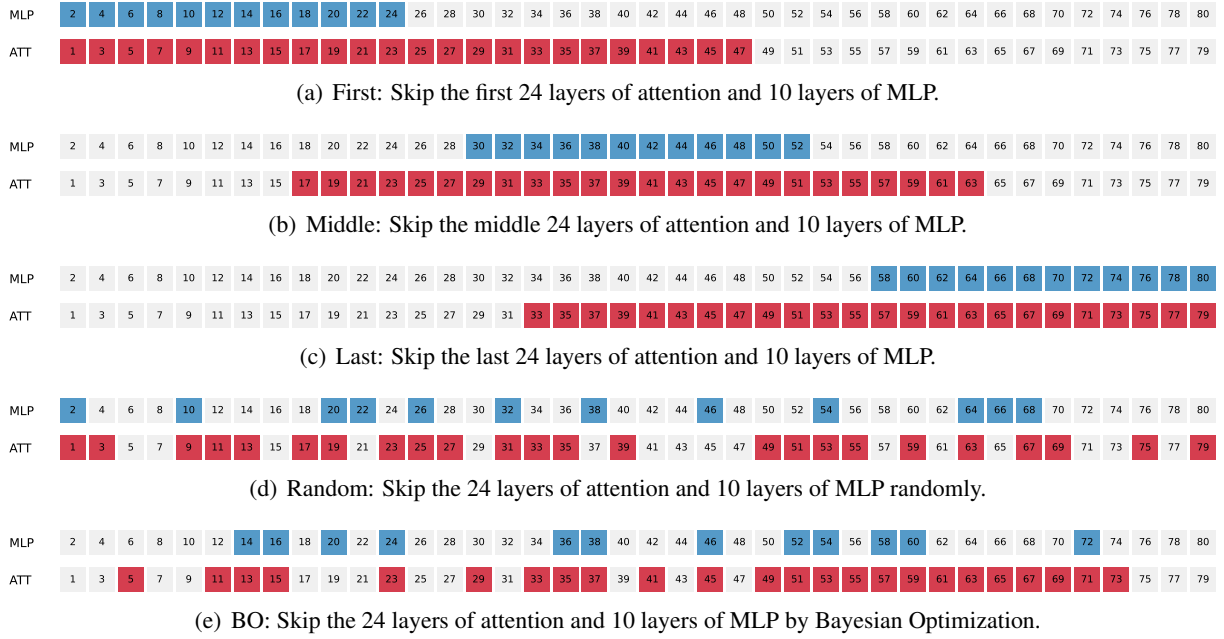


Figure 7: Visualization of layer skip distributions in LLaMA-2-13B using different strategies.

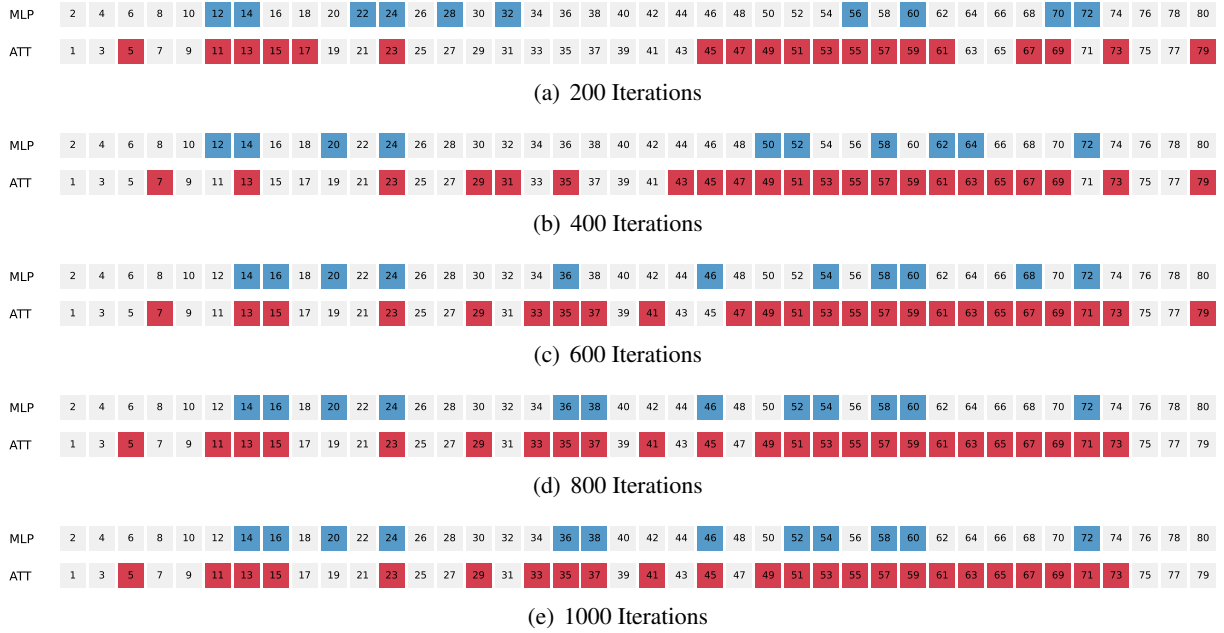


Figure 8: Visualization of LLaMA-2-13B layer skip distribution for different BO iteration numbers.

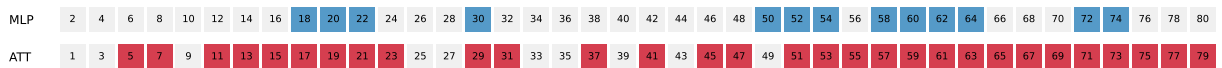


Figure 9: Visualize aggressive skip of 75% attention layers and 32.5% MLP layers of LLaMA-2-13B.

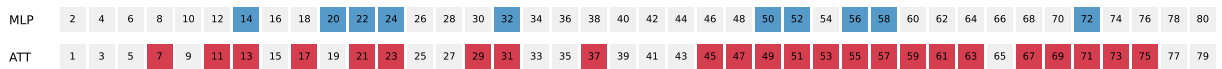


Figure 10: Visualization of layer skip distribution in LLaMA-2-13B for quantization and sparsification.